

Reworking the Tao–Mo exchange-correlation functional: II. De-orbitalization

H. Francisco

Quantum Theory Project, Dept. of Physics, University of Florida, Gainesville FL 32611, USA

A.C. Cancio

Dept. of Physics and Astronomy, Ball State University, Muncie IN 47306, USA

S.B. Trickey

*Quantum Theory Project, Dept. of Physics and Dept. of Chemistry,
University of Florida, Gainesville FL 32611, USA**

(Dated: orig. 14 July 2023; revised 27 Sept. 2023; 20 Oct. 2023)

In the preceding paper [1] we gave a regularization of the Tao–Mo exchange functional that removes the order-of-limits problem in the original Tao–Mo form and also eliminates the unphysical behavior introduced by an earlier regularization while essentially preserving compliance with the second-order gradient expansion. The resulting simplified, regularized (*sregTM*) functional delivers performance on standard molecular and solid state test sets equal to that of the earlier revised, regularized Tao–Mo (*rregTM*) functional. Here we address de-orbitalization of that new *sregTM* into a pure density functional. We summarize the failures of the Mejía–Rodríguez and Trickey de-orbitalization strategy (Phys. Rev. A **96**, 052512 (2017)) when used with both versions. We discuss how those failures apparently arise in the so-called z' indicator function and in substitutes for the reduced density Laplacian in the parent functionals. Then we show that the *sregTM* functional can be de-orbitalized somewhat well with a rather peculiarly parametrized version of the previously used deorbitalizer. We discuss, briefly, a de-orbitalization that works in the sense of reproducing error patterns but that apparently succeeds by cancellation of major qualitative errors associated with the de-orbitalized indicator functions α and z , hence is *not* recommended. We suggest that the same issue underlies the earlier finding of comparatively mediocre performance of the de-orbitalized TPSS functional. Our work demonstrates that the intricacy of such two-indicator functionals magnifies the errors introduced by the Mejía–Rodríguez and Trickey de-orbitalization approach in ways that are extremely difficult to analyze and correct.

I. CONTEXT

Meta-generalized gradient approximations (meta-GGAs) for the exchange-correlation energy in the Kohn–Sham formulation of density functional theory depend upon the electron number density $n(\mathbf{r})$, its spatial gradient ∇n , and, in most cases, on the positive-definite Kohn–Sham kinetic energy density

$$\tau_s = \frac{1}{2} \sum_i f_i |\nabla \varphi_i(\mathbf{r})|^2 \quad (1)$$

written in its explicitly orbital- and occupation-number-dependent form. The generic meta-GGA form is in terms

of the exchange enhancement factor F_x :

$$E_x^{mGGA}[n] = c_x \int d\mathbf{r} n^{4/3}(\mathbf{r}) F_x(s[n(\mathbf{r})], \tau_s(\mathbf{r})) \quad (2)$$

$$c_x := -\frac{3}{4} \left(\frac{3}{\pi} \right)^{1/3} \quad (3)$$

$$s := \frac{|\nabla n(\mathbf{r})|}{2(3\pi^2)^{1/3} n^{4/3}(\mathbf{r})}. \quad (4)$$

Corresponding dependencies, though not necessarily written the same way, can and do occur in meta-GGA correlation functionals E_c .

The explicit orbital dependence in Eq. (2) has a practical consequence that also is conceptually interesting. In principle, the Kohn–Sham exchange potential can be extracted as the functional derivative $v_x[n] = \delta E_x^{mGGA} / \delta n$. Doing so in practice is difficult because the functional dependence of the orbitals upon the density $\varphi[n]$ is not known explicitly, hence the optimized effective poten-

* francisco.hector@ufl.edu; trickey@ufl.edu

tial procedure must be used [2–4]. That procedure is sufficiently burdensome computationally that the common practice with meta-GGAs is to use the generalized Kohn-Sham procedure instead, with the orbital-dependent potential $v_x[\{\varphi\}] = \delta E_x^{mGGA}/\delta\varphi$. Ordinary KS and generalized-KS are the same for pure (i.e. orbital-independent) functionals but not for explicitly orbital-dependent ones [5].

That inequivalence is one motivation for pursuing orbital-independent counterparts of orbital-dependent meta-GGA functionals [6]. Having the KS (local) potential that is closely related to the g-KS orbital-dependent (non-local) potentials can provide insight into the workings of the functional. Another motivation is the fact that generalized-KS calculations are somewhat slower (at best) compared to most KS calculations. For a small number of calculations on modest sized systems, the speed difference may not matter but in the context of ab initio molecular dynamics on many (hundreds to thousands) condensed phases of large molecules (hundreds of electrons per molecule) the speed difference can be prohibitive. The challenge in that regard is to develop an orbital-independent meta-GGA functional which actually preserves that potential speed advantage.

Although one obviously could develop an orbital-independent meta-GGA functional from constraints and first principles, so far they actually have been developed by de-orbitalization of an orbital-dependent form. De-orbitalization replaces the τ_s dependence with a pure density functional dependent at most (for reasons of numerical tractability) upon $n(\mathbf{r})$, ∇n , and $\nabla^2 n$. The first two examples of which we are aware were Refs. 7, 8. A systematic scheme subsequently was put forth and applied by Mejía-Rodríguez and Trickey [6, 9, 10]. (Hereafter their approach is denoted “M-RT”.) They selected some promising approximate kinetic energy density functionals $\tau[n, \nabla n, \nabla^2 n] \approx \tau_s[n]$ and adjusted the parameters in them so as to give a good approximation to the iso-orbital indicator α widely used in meta-GGA X functionals. It is

$$\alpha[\{\varphi\}] := \frac{\tau_s - \tau_W}{\tau_{TF}} \quad (5)$$

$$\alpha_L[n, \nabla n, \nabla^2 n] \approx \alpha[\{\varphi\}] \quad (6)$$

The subscript “L” denotes a density-Laplacian dependence throughout this paper. The reference KE densities

are Thomas-Fermi and von Weizsäcker respectively

$$\tau_{TF} := c_{TF} n^{5/3}(\mathbf{r}) \quad (7)$$

$$c_{TF} := \frac{3}{10} (3\pi^2)^{\frac{2}{3}} \quad (8)$$

$$\tau_W := \frac{1}{8} \frac{|\nabla n(\mathbf{r})|^2}{n(\mathbf{r})}. \quad (9)$$

The chemical region indicator α has the important interpretive property that it is the enhancement factor in the expression for the Pauli contribution to the KS kinetic energy:

$$T_s[n] = T_W[n] + \int d\mathbf{r} \tau_{TF}[n] F_\theta[n] \quad (10)$$

$$F_\theta[n] \equiv \alpha[n]. \quad (11)$$

In some meta-GGA X functionals, a second chemical region indicator is used,

$$z := \frac{\tau_W}{\tau_s} \equiv \frac{5p}{5p + 3\alpha} \quad (12)$$

with $p := s^2$ and s given by Eq. (4). The fact that z is dependent upon α and that it has an order of limits problem, $\lim_{p \rightarrow 0} [\lim_{\alpha \rightarrow 0} z(\alpha, p)] \neq \lim_{\alpha \rightarrow 0} [\lim_{p \rightarrow 0} z(\alpha, p)]$, turns out to be both the reason for modifications of various two-indicator X functionals and for at least part of the problems with de-orbitalizing them.

A suggestion of that de-orbitalization difficulty appeared but was not investigated in Ref. 9. The two-indicator functional TPSS [11, 12] did not de-orbitalize very well with respect to standard molecular data set error patterns compared to the performance of de-orbitalized one-indicator meta-GGA X functionals.

The present work focuses on the most refined of the Tao-Mo family [13–15] of meta-GGA functionals, namely *rregTM*, [16] and our simplification of it, *sregTM*, presented in the preceding paper [1] (denoted hereafter as I). Motivation for considering *rregTM*, hence also for de-orbitalization of it, and the ensuing need for simplification is given in I. We begin this presentation by summarizing, in Sec. II, the key quantities in M-RT de-orbitalization and by giving a brief account of several variations of that strategy that fail for *rregTM*. We identify one source of the problem as being difficulty in reproducing z or its regularized modification z' (defined below and at Eqs. (14) and (22) in I) with de-orbitalizers that work for α . We trace that to the unphysical behavior of z' . Then, in Sec. III we apply the MR-T strategy in original and internally consistent versions to the *sregTM*

version introduced in I and show that it is reasonably successful except for molecular heats of formation. The partial success is dependent upon the parametrization of the deorbitalizer being done in a peculiar way, a matter not entirely understood. Despite the rather poor mean absolute deviation (MAD) for the molecular heat of formation, peculiarly, the de-orbitalized form in fact is reasonably successful in reproducing the MADs of the parent, orbital-dependent functional for molecular total energies or for atomic total energies. The problem with the molecular heat of formation MADs therefore is identified as a failure to have the same beneficial cancellation of error (between molecules and constituent atoms) in the de-orbitalized case as in the parent case. Interpretations and summary observations are in Sec. IV.

II. DIFFICULTIES DE-ORBITALIZING *rreg TAO MO*

Tao-Mo exchange functionals have the generic enhancement factor form

$$F_x^{TM}(p, z, \alpha) = w(z)F_x^{DME}(p, \alpha) + (1-w(z))F_x^{sc}(p, z, \alpha). \quad (13)$$

In *rregTM* and *sregTM* the indicator z is replaced by regularized forms, z' and z_{rev} respectively. In all cases, the switching function is

$$w(z) := \frac{z^2 + 3z^3}{(1 + z^3)^2} \quad (14)$$

with z , z' , or z_{rev} as appropriate. The intricate details of $F_x^{DME}(p, \alpha)$ and $F_x^{sc}(p, z, \alpha)$ are not needed for discussion of de-orbitalization; see I for those details.

Because α and z (and its regularized forms) are not independent, the M-RT approach de-orbitalizes α , then uses the second form of Eq. (12) or its regularized counterparts to generate the de-orbitalized z or regularized counterparts. The approach is motivated by recent progress in constructing F_θ forms, Eq. (11) for use in approximations in the Pauli kinetic energy in orbital-free density functional theory [17].

The deorbitalizers that were found in Refs. 6, 9, 10 to be particularly useful were denoted PC_{opt} , CR_{opt} , and TFL_{opt} . Detailed expressions for them are in Appendix A. Several aspects are relevant here. First, they all depend upon both the dimensionless reduced density gradient s and its square, p , [Eq. (4)] and upon the corre-

sponding reduced density Laplacian:

$$q := \frac{\nabla^2 n}{4(3\pi^2)^{2/3} n^{5/3}}. \quad (15)$$

Second, though all three deorbitalizers originated in the context of approximations to the Pauli kinetic energy, their original parametrizations do not satisfy Eq. (6) very well. In the original M-RT work that deficiency was addressed by optimizing the parameters against the $\alpha[\{\varphi\}]$ values generated from high-quality Hartree-Fock data for the first eighteen neutral atoms (in the central field approximation) [18, 19]. Those are the parameters associated with the “opt” part of the deorbitalizer names, e.g. PC_{opt} .

The M-RT procedure has had some notable successes (see, e.g. Ref. 6), but one may consider modified strategies. An internally consistent de-orbitalization, for example, would be to use the central field neutral atom orbitals from the targeted exchange-correlation functional (rather than Hartree-Fock orbitals).

To do that, code was written to generalize the Nelder-Mead [20] algorithm used previously to handle numerical orbitals. The internally consistent re-optimization was done using densities calculated with the *rregTM* exchange-correlation functional in NWChem-7.0.2 [21] for the first 18 neutral atoms with a UGBS basis set [22] and *xfine* grid setting as defined in that code. Error metrics on α_L such as Eqs. (39), (40), and (41) in Ref. 9, were used. Table I shows the original parameters and the internally consistent ones for *rregTM*. The new parameter values are rather insensitive to change in a relatively rich basis.

Table II compares the molecular test results for de-orbitalization of *rregTM* with both the internally consistent optimized parameters (“ PC_{new} ” etc.) and the original M-RT parameters (“ PC_{opt} ”, etc.). As usual, the tests are heats of formation according to Curtiss *et al.* [23, 24] for the 223 molecules of the G3X/99 test set, optimized bond lengths tested against the T96-R set [25, 26] and harmonic vibrational frequencies against the T82-F test set [25, 26]). Relevant molecular geometry information is provided in the respective publications of those test sets. To be clear, G3/99 test set results were calculated, as is conventional for that set, at the equilibrium geometries for the B3LYP DFA and 6-31G(2df,p) basis set and using B3LYP/6-31G(2df,p) zero-point energies (and thermal enthalpy corrections in the case of $\Delta_f H_{298}$) obtained with a frequency scale factor of 0.9854. Calcu-

TABLE I: Re-optimized (internally consistent from *rregTM* spherical densities) and original optimized parameters, denoted “new” and “opt” respectively, for the three M-RT deorbitalizers. Also shown are the PC_{rep} parameters determined with negative density Laplacian cutoff as discussed in Sec. III.

Functional	a	b
PC_{opt}	1.78472	0.25830
PC_{new}	1.79676	0.26444
PC_{rep}	1.50440	0.61565
TFL_{opt}	-0.20350	2.51390
TFL_{new}	0.00677	2.19899
Functional	a	b_1
CR_{opt}	4	-0.29549
CR_{new}	4	-0.31906
		2.61574
		2.61057

lations were done in NWChem-7.0.2 as described in I [1]. The calculations were self-consistent, pure KS for the orbital-independent functionals and generalized-KS for the orbital-dependent ones.

Compared to the original *rregTM*, the de-orbitalized performance clearly is a failure. Mean absolute deviations (MADs) for both heats of formation and frequencies from the de-orbitalized versions are much larger than for the original functional. While the internally consistent parametrization TFL_{new} , provides notable reduction in the MAD for heats of formation compared to TFL_{opt} outcomes, PC_{new} and CR_{new} yield no improvement for heats of formation, bond lengths, or harmonic frequencies over PC_{opt} and TFL_{opt} .

As an aside, we note that the results of both types of MR-T de-orbitalization applied to both the original Tao-Mo [13] and revised Tao-Mo [14] exchange-correlation functional were, generally, much poorer than those just shown for *rregTM*. We ascribe that worsened behavior to the order-of-limits difficulties in those two variants, hence did not pursue their de-orbitalization further. Similarly, we now suspect that the order-of-limits problem in the original TPSS functional contributed to the somewhat disappointing de-orbitalization results found in Ref. 9 but have not investigated that suspicion.

Results for the solid test data bases used in I [27–29] (from VASP calculations; technical details as in I and symmetries as tabulated in Ref. 10) with these two de-orbitalizations were essentially as poor as what is shown in Table II for molecules.

Puzzled, we attempted several rather straightforward

refinements of optimization of the deorbitalizers and of the numerical techniques. That included use of both α and z or z' in the optimization of the deorbitalizers, changing the relative weights of the two in the de-orbitalization metric, enriching basis sets, comparing molecular data set results from our local implementation of *rregTM* against the implementation in LibXC-5.1.7 [30], optimization of deorbitalizers based on energy difference metrics, e.g. $|E_{xc,orig} - E_{xc,deorb}|$ or of a separate deorbitalizer for exchange (with metric on z') and for correlation (with metric on α), etc. We also considered optimization of a de-orbitalized $w(z')$. To ascertain that the molecular behavior was not, somehow, special, we tried several of those de-orbitalization options on the solid data sets [27–29] (symmetries as tabulated in Ref. 10 with VASP-5.4.4 [31], using both PAWs and ultra-soft pseudopotentials. (Procedural details for VASP are in I.) There were only small differences compared to the molecular studies. Qualitatively and quantitatively, the outcomes uniformly were poor.

Painstaking analysis leads to the conclusion that the failure stems mostly from a combination of three factors. One is the unphysical behavior of z' discussed in detail in I. In summary, $z \geq 0$ by definition (see Eq. (12)) but the regularization of z into z' introduces spurious negative behavior. The Supplemental Information [32] provides plots for two molecules that are examples of that behavior. In one of those examples (BeH), the unphysical behavior of z' is manifested explicitly in the deorbitalized z'_L .

Second, z is not as simply related to the Pauli or Kohn-Sham kinetic energy densities as is α . Recall that α is intrinsically the Pauli KE enhancement factor, see Eq. (11), whereas z is non-linearly related to it. The non-linear dependence of z' upon α is much more intricate than for z . The practical consequence is that deorbitalizer forms derived from orbital-free KE studies that can be made to fit α reasonably well, nevertheless can introduce important errors in deorbitalizing z or z' . We show this for the cases of single and triple bonds in the two molecules C_2H_2 and C_3H_4 in Fig. 1 for α and its de-orbitalization and Fig. 2 for z' and its de-orbitalization. (The C_3H_4 geometry used is propyne, $H_3-C-C-H$, as in Ref. 33.) The dramatic difference in the fidelity of the de-orbitalized α to its parent and the de-orbitalized z' is obvious. The de-orbitalized z' has a strange jagged oscillation along each C-H bond in C_2H_2 and large, spurious oscillations in the C_2 single bond compared to relatively

TABLE II: Results of the de-orbitalized version, *rregTM-L*, of the *rregTM* XC functional using the re-optimized parameters from Table I (upper half) vs. de-orbitalized with the original M-RT parameters (lower half). The Def2-TZVPP basis and xfine grid setting were used in NWChem. Heat of formation errors (mean error = “ME”, mean absolute deviation = MAD”) in *kcal/mol*, bond length errors in Å, and frequency errors in *cm*⁻¹.

		<i>PC</i> _{new}	<i>TFL</i> _{new}	<i>CR</i> _{new}	<i>rregTM</i>
Heats of Formation	ME	14.106	16.165	20.089	-3.790
	MAD	16.964	18.843	22.777	5.612
Bonds	ME	0.020	0.021	0.022	0.012
	MAD	0.022	0.022	0.024	0.014
Frequencies	ME	-49.684	-46.570	-50.159	-21.011
	MAD	55.942	51.950	55.224	35.578
		<i>PC</i> _{opt}	<i>TFL</i> _{opt}	<i>CR</i> _{opt}	
Heats of Formation	ME	14.527	21.270	19.527	-3.790
	MAD	17.385	23.656	22.259	5.612
Bonds	ME	0.020	0.021	0.021	0.012
	MAD	0.022	0.024	0.024	0.014
Frequencies	ME	-50.152	-49.321	-49.652	-21.011
	MAD	56.391	55.528	55.519	35.578

accurate behavior at the center of the C₂ triple bond in C₃H₄. The equally spurious jagged oscillation along the C-H bond shows up again. We do not worry too much about the misbehavior well beyond the molecular ends because of the density decay, but the misbehaviors in critical bonding regions are unignorable signs of trouble.

To show the consequences, Fig. 3 gives an example of the original $w(z')$ compared to evaluation with a typical de-orbitalization of z' . Unsurprisingly, all of the deficiencies of the de-orbitalized z' persist in $w(z')$. What is evident is that a deorbitalizer for z' together with α must have greater flexibility in its form than for α alone. The challenge of devising such a form is made more severe by the nonlinear character of $w(z)$.

Third is a bit of unintended nearly circular reasoning in the de-orbitalization of some meta-GGA X functionals including the TM family. The reduced density Laplacian q diverges at nuclear sites if the density has a true Kato cusp and very spiky behavior if the cusp is approximated in a finite Gaussian basis. To avoid that, the *rregTM* X replaces q with an orbital-dependent approximation,

$$\tilde{q}(\alpha, p) := \frac{9}{20}(\alpha - 1) + \frac{2}{3}p. \quad (16)$$

See Eq.(18) in I. This yields a smoothly varying function which approaches q in the limit of slowly varying density.

But M-RT deorbitalization uses an approximation to $\tilde{q}(\alpha, p)$ generated from a q -dependent approximation to α , namely $\alpha_L(p, q)$. Thus it reintroduces q -dependence in an expression built intentionally to remove q . The full consequences of that reintroduction are not easy to discern.

Figure 4 illustrates the issue. It shows q and $\tilde{q}(\alpha, p)$ for C₂H₂ and C₃H₄. For both, the most significant difference between these quantities lies in the atomic nuclei region, where q exhibits sharp negative peaks of considerable magnitude. By design, those peaks do not appear in \tilde{q} , which shows slightly negative regions there. In the bonding regions, both functions are relatively close in value.

Implicit in this is a challenge for the M-RT deorbitalization. Its parametrization of α must be such that \tilde{q}_L reproduces \tilde{q} , not q . That includes smoothing such that the spikes from the q -variable do not appear in \tilde{q}_L . Moreover, the weakly varying limit of the de-orbitalized quantity, $\tilde{q}_L(p, q) \rightarrow q$ must be preserved in the face of complicated nonlinear dependence on q itself through the deorbitalized α . Note that the figure shows that near bond centers, where $p \rightarrow 0$, \tilde{q}_L seems to meet that behavior rather well. Of course, the deorbitalized \tilde{q}_L also must reproduce \tilde{q} (not q) for larger values of p .

The difficulty that is hard to analyze is the effect

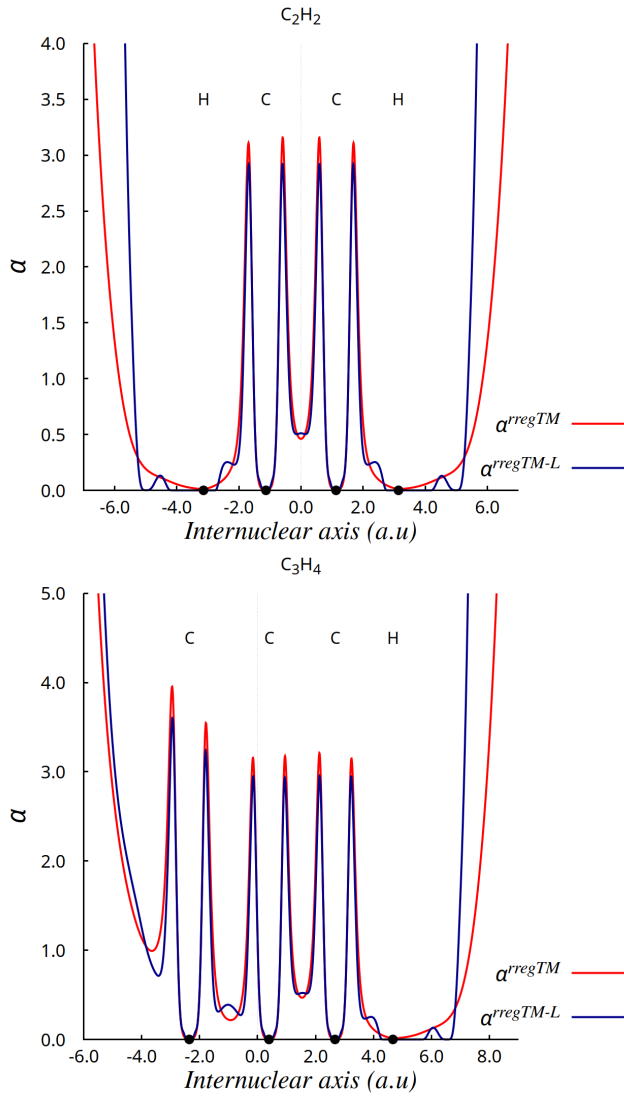


FIG. 1: Orbital-dependent α and its de-orbitalized approximation from PC_{new} for distinct bonding types, C_2H_2 (upper) and C_3H_4 (lower). The plots are along the molecular axis.

of these competing requirements upon parametrization, which is done on α , not on \tilde{q} . We have some evidence that these competing requirements are a significant contributor to the limitations on de-orbitalization performance already presented. See discussion in Sec. IV regarding a changed parametrization, called PC_{rep} that is strongly affected by the structure of q . Further on, we have some discussion on parametrization of the deorbitalizer that works for molecules but breaks compliance with the gradient expansion in the slowly varying limit. \tilde{q}_L does not go to q in that case.

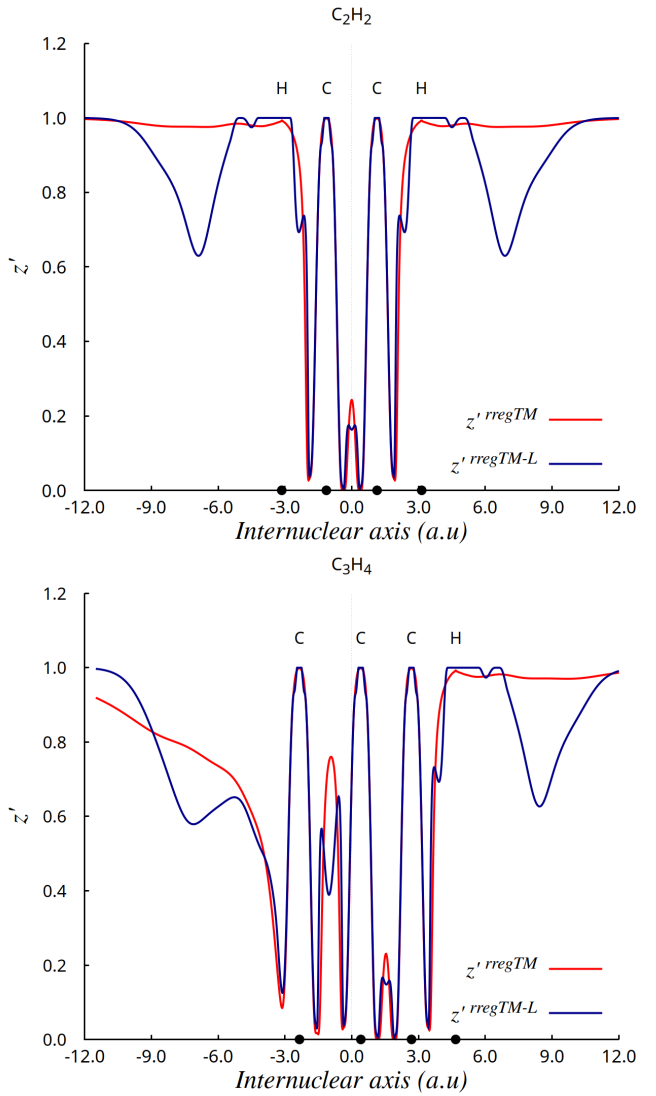


FIG. 2: As in Fig. 1 for orbital-dependent z' and its de-orbitalized approximation from PC_{new} .

III. DE-ORBITALIZING SIMPLIFIED REGULARIZED TAO-MO *sreg* TM

Motivated by the misbehavior just discussed (as well as other issues), in I we presented a simplified regularization of Tao-Mo exchange, *sreg*TM E_x . Distinct from the *rreg*TM functional, *sreg*TM has a regularized z variable that is properly positive semi-definite, $z_{rev} \geq 0$, and that has a simple regularization constant rather than the function used in *rreg*TM. We showed in I that *sreg*TM E_x works well with the *rreg*TM correlation (which is a refinement of SCAN correlation [34, 35]) on standard test sets and about as well with original PBE correlation (with fixed β parameter) [36]. The second combination is interesting because it simplifies the correlation term to a

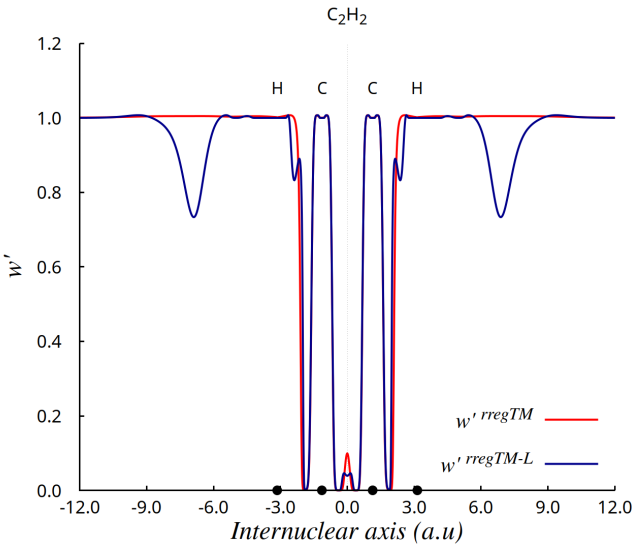


FIG. 3: As in Fig. 1 for orbital-dependent $w(z')$ and its de-orbitalized approximation from PC_{new} .

GGA, which can help both computational speed and stability.

For the de-orbitalization we focused on the *v2-sregTM* variant (recall I). We chose it rather than *v1-sregTM* because *v2-sregTM* uses only α and z_{rev} whereas *v1-sregTM* also uses the original z . The two variants yield essentially indistinguishable test results, so we chose the simpler one. As shown in Part I, that consistent use of z_{rev} in *v2-sregTM* also leads to its near compliance with the second-order gradient expansion in the limit of a slowly varying density. Inconsistency in *v1-sregTM* leads to poorer behavior in that limit.

Because *sregTM* exchange has a different regularization of z than *rregTM*, it seemed opportune to revisit the de-orbitalization parameters. In addition to

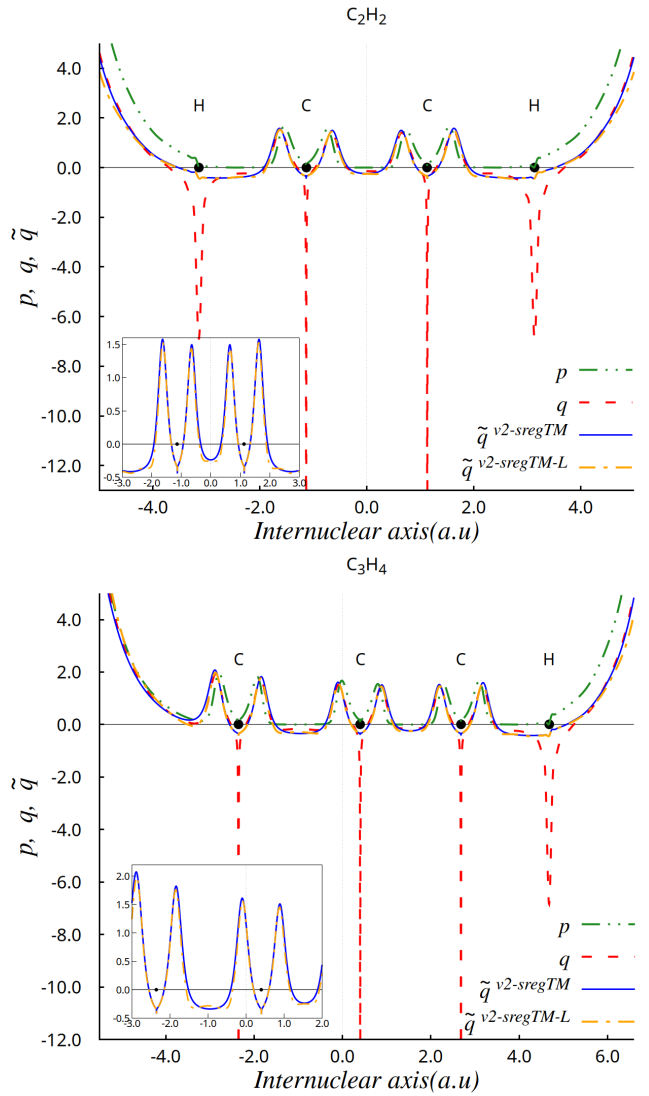


FIG. 4: p and q from *v2-sregTM* densities along with \tilde{q} and its deorbitalized approximation \tilde{q}_L from PC_{rep} with their respective densities for C_2H_2 (upper) and C_3H_4 (lower). The plots are along the molecular axis. The insets compare \tilde{q} and \tilde{q}_L around the C atoms for C_2H_2 and the leftmost two C atoms for C_3H_4 .

the reparametrization discussed in Sect. I therefore, we also did a distinctly different one. We considered $PC(s, qH(q))$, where the notation indicates that the Perdew-Constantin form was used with the variable q restricted to positive values by multiplication with the Heaviside unit step function $H(q)$. This constraint was introduced in the parametrization (only) for numerical investigation of the consequences of $q < 0$. Pragmatically, it turns out to be a useful parametrization constraint; see brief discussion below. This reparametriza-

tion used the error measure $\Delta_\alpha + \Delta_{z_{rev}}$ with

$$\Delta_{z_{rev}} = \sum_{i=1}^M \frac{1}{N_i} \int d\mathbf{r} n_i |z_{rev}[n_i] - z_{rev}^{approx}[n_i]|. \quad (17)$$

The parameter re-optimization was done as before, using densities calculated with the combination X-*v2-sregTM*+C-*rregTM* in NWChem-7.0.2 for the first 18 neutral atoms with the **xfine** grid setting as defined in that code. Testing showed that we did not need the very large basis set used in the work reported above, so we reverted to the Def2-TZVPP basis [37]. The resulting parametrization, named PC_{rep} , has parameter values $a = 1.50440$ and $b = 0.61565$. Observe that these are substantially different from the values for PC_{opt} and PC_{new} shown in Table I.

Figures 5 and 6 display the X enhancement factor behavior of the *sregTM* functional and its corresponding deorbitalized version *v2-sregTM-L* with PC_{rep} for C_2H_2 and C_3H_4 . The de-orbitalized enhancement factors align reasonably closely with those of the parent counterpart except for some modest oscillations in the bonding regions. Comparable behavior is evident in the X enhancement factors for *rregTM* and *rregTM-L*(PC_{new}); see the Supplementary Information.

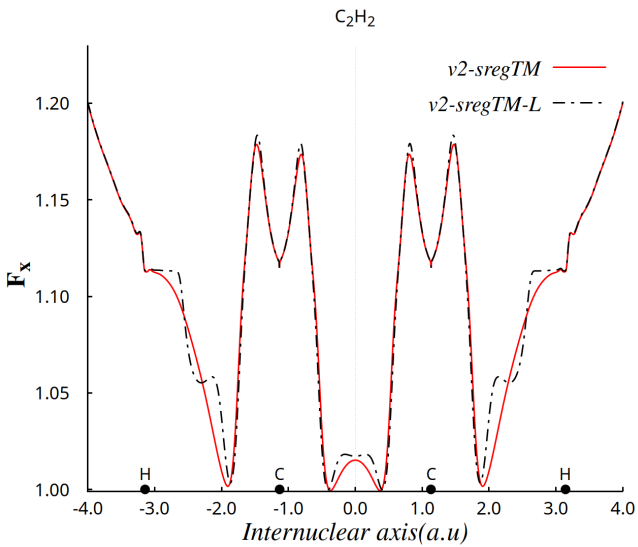


FIG. 5: Enhancement factor F_X for *v2-sregTM* and *v2-sregTM-L* (PC_{rep}) functionals for the C_2H_2 molecule.

Next we give performance statistics for the de-orbitalization of the *v2-sregTM* variant (recall I and discussion above). We did the de-orbitalization in conjunction with *regTM* correlation. (For results of de-

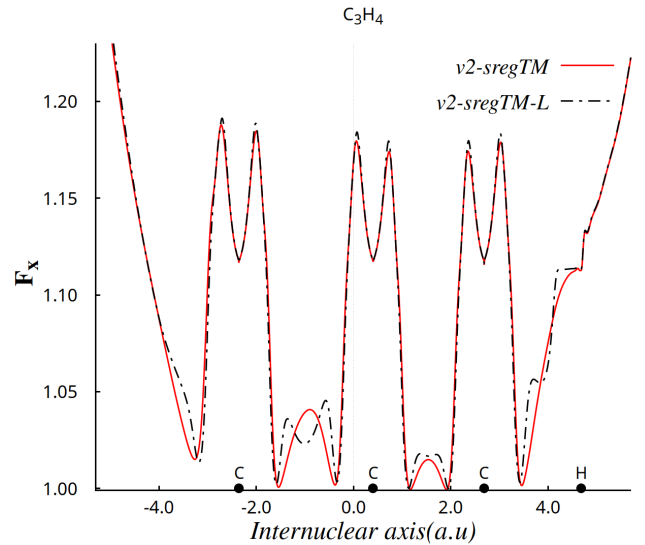


FIG. 6: As in Fig. 5, but for the C_3H_4 molecule.

orbitalization of *v2-sregTM-L* X plus PBE C with PC_{rep} de-orbitalization, and brief discussion see the Supplemental Information.)

As before, we used NWChem 7.0.2 and VASP-5.4.4 with the procedures and parameter choices as in I. To assess the fidelity of de-orbitalization relative to *v2-sregTM*, again we used the same molecular and solid-state test sets as in Part I.

Detailed results are tabulated in the Supplemental Information [32]. Tables III and IV respectively show the performance against the molecular and solid data sets for the de-orbitalized combination of *v2-sregTM* with *rregTM* correlation. Observe that the deorbitalizer common to both Tables is PC_{rep} . (As an aside, note that the poor performance of CR and TFL variants in de-orbitalizing *rregTM* discussed above persists in the case of de-orbitalizing *v2-sregTM*, so we do not report those results.) For the molecular tests only, however, we also show the results of straightforward M-RT deorbitalization of *v2-sregTM*, that is, with PC_{opt} . Comparison with the results of original M-RT deorbitalization presented in Table II shows that in going from z' in *rregTM* to z_{rev} in *v2-sregTM* the M-RT deorbitalization actually worsened. Then the shift in parameters to PC_{rep} makes a dramatic improvement in molecular heats of formation error. Even so, that version of *v2-sregTM-L* is not as good as its parent functional on heat of formation MAD, about the same on bond length MAD, and better on harmonic frequencies. The heat of formation performance again is somewhat reminiscent of what was found with

the M-RT de-orbitalization of TPSS [9].

The improvement on going from PC_{opt} to PC_{rep} parametrization is not as dramatic in the case of the solids. Nevertheless, $v2\text{-}sreg$ TM-L outperforms $rreg$ TM-L on them. In detail, the MADs for lattice constants and bulk moduli from $v2\text{-}sreg$ TM-L are not as good as for the parent $v2\text{-}sreg$ TM. Unlike the molecular case, the cohesive energy MADs are essentially identical. The KS band gap MAD is worse but that is expected. For $v2\text{-}sreg$ TM-L what is shown is a true KS band gap (local potential) whereas it is not for $v2\text{-}sreg$ TM (generalized KS).

Clearly the molecular heat of formation error induced by de-orbitalization is large, with the MAD for the de-orbitalized functional about twice that for the parent. This is striking in light of the fact that the solid cohesive energy MADs for the parent and de-orbitalized functionals are essentially identical. The difference can be diagnosed as a difference of cancellation of errors. For the G3 molecular data set, the mean absolute relative error (MARE: $\sum_i |[E_i - E_{L,i}]/E_i|$, with E_i the relevant molecular energy from the parent functional and $E_{L,i}$ from the de-orbitalized functional) for the molecular total energy from $v2\text{-}sreg$ TM-L is 0.06554 while from r^2 SCAN-L it is 0.09195 [6]. For the G3 atomic total energies, the comparison is 0.00514 versus 0.00905. From these, one might expect that $v2\text{-}sreg$ TM-L atomization energy MARE (thus, also for heat of formation) also would be superior to the r^2 SCAN-L result. Yet in reality, the situation is reversed for the G3 atomization energies. The MARE for $v2\text{-}sreg$ TM-L is 4.2303 while for r^2 SCAN-L it is 2.6444. Apparently, the $v2\text{-}sreg$ TM-L error pattern on the G3 molecules differs significantly from that on the constituent atoms, so that the kind of beneficial cancellation that often comes with DFAs, including with r^2 SCAN-L, does not occur.

This is consistent with what we find in the solid cohesive energies which have very good MAD. That data set is dominated by elemental solids with a few diatomics, whereas the G3/99 set is light to medium inorganic and organic molecules. The diagnosis of limited error cancellation also is consistent with a test in which we recalculated the G3/99 heats of formation using a large unit cell and PAWs in VASP. That did not alter the G3/99 heat of formation MAD shift from parent $v2\text{-}sreg$ TM to de-orbitalized $v2\text{-}sreg$ TM-L meaningfully. Yet the two calculations are quite different, all-electron versus plane-wave with PAW cores. One expects core-state cancellation to be strong in both cases, so the deduction that the

valence energetics error pattern from $v2\text{-}sreg$ TM-L in the molecules differs substantively from that in the atoms is supported.

The MAD data in Tables III and IV suggest that the electronic forces on the nuclei near equilibrium may be less sensitive to de-orbitalization than the other quantities. Though the molecular bond length and lattice constant MADs increase by about 33% upon de-orbitalization by PC_{rep} , those are shifts in small absolute errors. They are significantly better than PBE length MADs (see data in I). In contrast, the MAD shifts upon de-orbitalization in heats of formation, cohesive energy, frequencies, etc. are similarly large fractions of rather large errors. This comparative insensitivity suggests that the electronic forces from the de-orbitalized $v2\text{-}sreg$ TM-L are reasonable.

The Supplementary information provides tabulations showing that the total number of NWChem SCF steps required for each of the three molecular test sets for both parent and de-orbitalized versions of $v2\text{-}sreg$ TM and $rreg$ TM. The two parent functionals are essentially identical. In both cases, $v2\text{-}sreg$ TM versus $v2\text{-}sreg$ TM-L and for $rreg$ TM versus $rreg$ TM-L the step count is higher for the deorbitalized versions than the parent functionals. This outcome is not wholly surprising given experience with numerical instabilities caused by the density Laplacian. For the heat of formation, the increment is about 11%. Thus, any improvement in time per step for the de-orbitalized case relative to the original gKS case greater than 10% would give a net gain in performance.

The remaining comparison is magnetization. Figs. 7, 8, and 9 show the fixed spin moment energy as a function of magnetization for bcc Fe, fcc Co, and fcc Ni as calculated from the PBE, $rreg$ TM, $v2\text{-}sreg$ TM, and $v2\text{-}sreg$ TM-L functionals. Table V gives the saturation magnetizations. Generally the de-orbitalization from $v2\text{-}sreg$ TM to $v2\text{-}sreg$ TM-L sustains or slightly alters the saturation magnetization. For Fe, it is a small underestimate, but there are small overestimates for Co and Ni. Details of the magnetization energetics are tabulated in the Supplemental Information. Gratifyingly, the $v2\text{-}sreg$ TM-L preserves the good elemental magnetization properties of both its parent $v2\text{-}sreg$ TM and its antecedent, $rreg$ TM.

TABLE III: Molecular test results summary for the de-orbitalized version, $v2\text{-}sreg\text{TM-L}$, with the PC_{rep} deorbitalizer, of the $v2\text{-}sreg\text{TM}$ XC functional. For comparison, results from original M-RT type de-orbitalization with PC_{opt} are shown. The Def2-TZVPP basis and xfine grid setting were used in NWChem. Heat of formation errors in kcal/mol , bond length errors in \AA , and frequency errors in cm^{-1} .

		<i>rregTM</i>	<i>v2-sregTM</i>	<i>v2-sregTM-L (PC_{opt})</i>	<i>v2-sregTM-L (PC_{rep})</i>
Heats of Formation	ME	-3.790	-3.512	23.328	8.675
	MAD	5.612	5.895	23.956	11.471
Bonds	ME	0.012	0.013	0.020	0.014
	MAD	0.014	0.015	0.021	0.017
Frequencies	ME	-21.011	-19.275	-36.060	-32.277
	MAD	35.578	34.272	43.934	43.499

TABLE IV: As in Table III for solid test results for $v2\text{-}sreg\text{TM-L}$ done with PC_{rep} . Equilibrium lattice constant errors in \AA , cohesive energy errors in eV/atom , bulk modulus errors in GPa , and Kohn-Sham band gap errors in eV .

		<i>rregTM</i>	<i>v2-sregTM</i>	<i>v2-sregTM-L(</i> PC_{rep} <i>)</i>
Lattice Constants	ME	0.000	0.004	0.018
	MAD	0.029	0.031	0.041
Cohesive Energies	ME	0.212	0.159	0.010
	MAD	0.251	0.216	0.205
Bulk Moduli	ME	1.856	0.223	-3.265
	MAD	6.740	6.602	8.747
KS Band Gaps	ME	-1.52	-1.53	-1.73
	MAD	1.52	1.53	1.73

TABLE V: Magnetic moments in μ_B for three elemental $3d$ solids as determined from different XC functionals.

Exp. refers to the experimental data [38, 39].

	Exp.	<i>rregTM</i>	<i>v2-sregTM</i>	<i>v2-sregTM-L</i>	<i>PBE</i>
				(PC_{rep})	
Fe	2.22	2.10	2.17	2.15	2.18
Co	1.72	1.72	1.73	1.75	1.64
Ni	0.62	0.68	0.66	0.69	0.63

IV. CONCLUDING REMARKS

To summarize, exhaustive study of procedural and technical variations shows convincingly that straightforward use of the M-RT de-orbitalization strategy on *rregTM* and *sregTM* does not work. The complicated dependence of the *rregTM* and *sregTM* X functionals upon two indicator functions that are not independent makes diagnosis of the cause (or causes) of that failure

very difficult. Numerical exploration and visualization therefore become more helpful than they would be in a less opaque context.

It is worth re-emphasizing a particular kind of structural complexity that occurs in the TM family of X functionals (and some other meta-GGAs as well) that we have mentioned already but that is a previously undiscussed difficulty for M-RT de-orbitalization. The issue is elimination of the reduced density Laplacian q (that arises in the gradient expansion) in any part of the X functional. The motivation is to remove the spikiness discussed already and to avoid fourth spatial derivatives in the X potential. As discussed above, in *rregTM*, the ingredient enhancement factor $F_x^{sc}(p, \alpha)$ (see Part I, Eq. (17)) by replaces q with is $\tilde{q}(\alpha, p)$ in Eq. (16). The explicit orbital dependence re-introduced by α then must be removed in de-orbitalization by use of an approximate, orbital-free $\alpha_{approx}[p, q]$. In essence

$$q \rightarrow q_{approx}[\alpha, p] \rightarrow q_{approx}[\alpha_{approx}[p, q], p]. \quad (18)$$

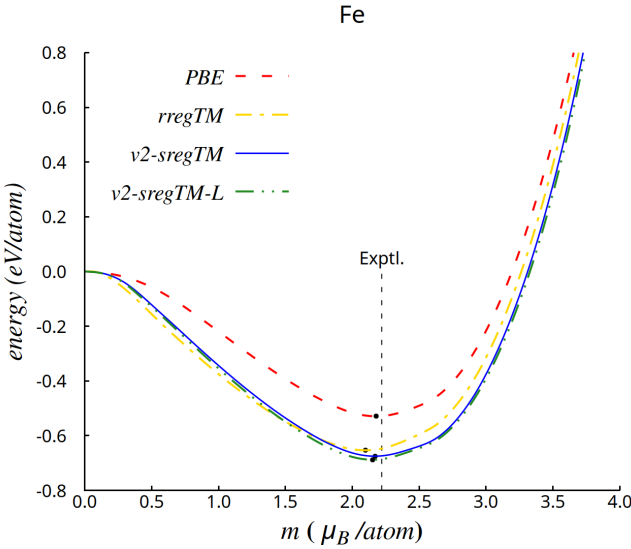


FIG. 7: Fixed spin moment energy on a per-atom basis for bcc Fe from four XC functionals using the calculated equilibrium lattice parameters.

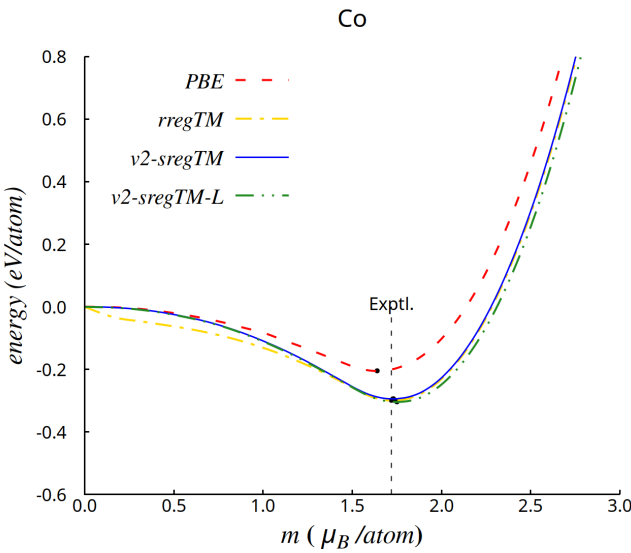


FIG. 8: As in Fig. 7 for fcc Co.

This provides the basis for a plausible interpretation of the success of the $p, qH(q)$ re-parametrization, PC_{rep} . The reasoning is that as long as $\alpha_L(p, q)$ is well-behaved, the ensuing $\tilde{q}(p, \alpha_L)$ will be also, with the spikiness from q suppressed. Given that smoothness, one then can exempt the parametrization from having to include $q < 0$ contributions, which changes the parametrization error minimization qualitatively. The result is apparent. The parameter values change dramatically, PC_{rep} ($a = 1.50440$, $b = 0.61565$), compared to the internally consistent version of the M-RT procedure, PC_{new} ($a = 1.79676$,

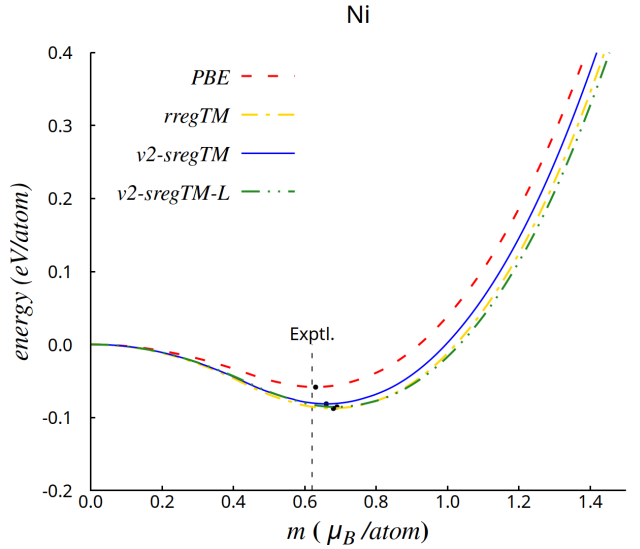


FIG. 9: As in Fig. 7 for fcc Ni.

$b = 0.26444$; recall Table I). These make a substantial improvement in the performance of de-orbitalized $v2$ - $sregTM$ -L relative to what is obtained from use of PC_{new} . Recall Table I.

For diagnosis, we did, in fact, try an even more brutal approximation than the $q < 0$ cutoff used in determining PC_{rep} , namely to use that constraint in the molecular and solid calculations also. Note that we do *not* recommend this brutal approximation. Numerically the heat of formation MAD results are improved quite a bit. But visualization of the $v2$ - $sregTM$ -L functions z_{rev} and $w(z_{rev})$ shows that they are drastically and strangely different from the corresponding functions for the parent functional. The differences are so gross that the orbital-independent functional is better understood as being a separate, quite peculiar construction, not a de-orbitalization. The improvement in G3/99 heat of formation MAD (relative to $v2$ - $sregTM$ -L) that it gives apparently comes from very uneven redistribution of error in the α function: modest for atoms, and dramatic, particularly for covalent bonds and near hydrogens, in molecules. Thus there is fortuitous error cancellation that is missing from ordinary M-RT de-orbitalization, and what may be a clue for constructing a more disciplined post-deorbitalization functional.

Also note that if we were to use the pure PC form, then by construction the resulting \tilde{q}_L would reduce to q in the slowly varying limit. It is the reparametrizations used in PC_{opt} and likely PC_{rep} that are problematical in this limit. They produce models of α that do not

comply with its gradient expansion for small p and q [40]. However, these reparametrizations are necessary for practical success in real systems.

The circularity in q does not show up in functionals such as MVS [41], SCAN [34, 35], or r^2 SCAN because they depend only on α and that dependence is only in the switching function between two X functionals. The independence of the component exchange functionals from α and its use only in switching suggests an alternative approach to the M-RT scheme, albeit a quite different one. It would be to build a new version of Tao-Mo exchange that included reproduction of the behavior of $\tilde{q}(\alpha, p)$ with a function of p and q . This would include reducing to q itself in the slowly varying limit. As discussed at the outset, such an approach is really the construction of orbital-free functionals from the outset, not de-orbitalization, so it is outside the scope of the present work.

Whether there are even better parameters within the M-RT approach is not easy to discern. No systematic way to make a more effective search using atomic calculations only (to avoid all fitting to any bonded system) is apparent. Better de-orbitalizer forms also are hard to construct.

The issue may be compounded by the nature of z' diagnosed in I. There we noticed (Fig. 1) that z' for $rregTM$ is a peculiarly complicated function in the limit $p \approx 0$ typical of covalent bonds. In particular, in order to accommodate $z' = 1$ for a single-orbital system ($\alpha = 0$) and $z' = 0$ for the homogeneous electron gas ($\alpha \approx 1$), the function z' varies sharply as a function of α . And $\alpha < 1$, as well as p small, is the signature of covalent bonding. Thus errors of the sort discussed above in α become amplified in z' in a way that is not easy to remove for energetically important situations. Switching to the regularization in z_{rev} mitigates this difficulty.

A related aspect of the reparametrization has been evident since the first M-RT paper [9]. An expression that works well as a de-orbitalizer does not necessarily work well as the integrand of a kinetic energy density functional (and conversely). The problem is the gauge ambiguity of any KEDF τ_s : $T_s[n] = \int d\mathbf{r}(\tau_s[n(\mathbf{r})] + D[n(\mathbf{r})])$ for all $D[n(\mathbf{r})]$ such that $\int d\mathbf{r}D[n(\mathbf{r})] = 0$ on the relevant domain. This is one reason for reparametrization. Since KEDF development is not the focus of this research we have not investigated whether, for example, PC_{rep} is a good KEDF. Conversely, KEDF progress does not necessarily translate into a better de-orbitalizer.

Finally, the PC_{rep} de-orbitalization of $v2\text{-}sregTM$ does

provide a reasonable comparison of molecular total energies relative to one another but not heats of formation. On bond lengths it is reasonable and, like other de-orbitalized meta-GGAs [6, 9] fair on molecular frequencies. For solids it is as good on standard data sets relative to its parents as other de-orbitalized meta-GGAs [6, 10]. The good magnetization behavior of the parent orbital-dependent functional $v2\text{-}sregTM$ is preserved in $v2\text{-}sregTM\text{-L}$, unlike the de-orbitalizations of SCAN and r^2 SCAN that actually perform better than their parents [6, 42].

V. SUPPLEMENTARY MATERIAL

The Supplemental Information [32] provides MAD results for use of PBE correlation with $v2\text{-}sregTM\text{-L}$, graphical comparisons of X enhancement factors for original and de-orbitalized versions of $rregTM$ in the C_2H_2 and C_3H_4 molecules, atomic X potentials for two different de-orbitalizations, plots of two cases in which the earlier regularization z' has unphysical behavior ($z' < 0$), detailed results on $3d$ elemental magnetization, and comparative information on the number of SCF steps. There also is system-by-system tabulation of results for each of the molecular and crystalline test sets.

Acknowledgment We acknowledge several helpful conversations with Daniel Mejía Rodríguez and suggestions from Angel Albavera-Mata with thanks. Work supported by U.S. National Science Foundation grant DMR-1912618.

VI. AUTHOR DECLARATIONS

Conflict of Interest - The authors have no conflicts to disclose.

Author Contributions

Héctor Francisco: Conceptualization (equal); Data curation (lead); Formal analysis (supporting); Investigation (lead); Methodology (lead); Software (lead); Validation (lead); Writing – review and editing (supporting).

Antonio C. Cancio: Conceptualization (equal); Data Curation (equal); Formal analysis (equal), Funding acquisition (supporting); Methodology (equal); Project administration (supporting); Software (equal); Supervision (equal); Validation (equal); Visualization (lead); Writing – original draft (supporting); Writing – review and editing (equal).

S. B. Trickey: Conceptualization (equal); Data Curation (supporting) Formal analysis (equal); Funding acquisition (lead); Investigation (supporting); Methodology (equal); Project administration (lead); Resources (lead); Supervision (lead); Validation (equal); Writing – original draft (lead); Writing – review and editing (equal).

Data Availability: The data that supports the findings of this study are available within the article and its supplementary material.

Appendix A: Deorbitalizers

PC_{opt}

The original *PC* kinetic energy density functional [8] is based on a modified fourth-order gradient expansion (MGE4) that has the enhancement function form

$$F_{\theta}^{\text{MGE4}} = \frac{F_{\theta}^{(0)} + F_{\theta}^{(2)} + F_{\theta}^{(4)}}{\sqrt{1 + [F_{\theta}^{(4)} / (1 + F_{\theta}^W)]^2}}. \quad (\text{A1})$$

The ingredient quantities are

$$F_{\theta}^{(0)} := 1 \quad (\text{A2})$$

$$F_{\theta}^{(2)} := \frac{5}{27}s^2 + \frac{20}{9}q \quad (\text{A3})$$

$$F_{\theta}^{(4)} := \frac{8}{81}q^2 - \frac{1}{9}s^2q + \frac{8}{243}s^4 \quad (\text{A4})$$

$$F_{\theta}^W = \frac{5}{3}s^2. \quad (\text{A5})$$

PC and PC_{opt} interpolate between the MGE4 form and the von Weizsäcker lower bound, F_{θ}^W ,

$$\Theta_{\text{PC}}(\xi) = \begin{cases} 0, & \xi \leq 0 \\ \left[\frac{1+e^{a/(a-\xi)}}{e^{a/\xi}+e^{a/(a-\xi)}} \right]^b, & 0 < \xi < a \\ 1, & \xi \geq a \end{cases} \quad (\text{A6})$$

The *PC* form thus is

$$F_{\theta}^{\text{PC}} = F_{\theta}^W + z^{\text{PC}} \Theta_{\text{PC}}(z^{\text{PC}}) \quad (\text{A7})$$

with

$$z^{\text{PC}} = F_{\theta}^{\text{MGE4}} - F_{\theta}^W. \quad (\text{A8})$$

The original *PC* parameter values are $a = 0.5389$, $b = 3$. The PC_{opt} values are $a = 1.784720$, $b = 0.258304$ [9].

CR_{opt}

The *CR* mGGA enhancement function [33, 43] is

$$F_{\theta}^{\text{CR}} = 1 + F_{\theta}^W + \xi^{\text{CR}} \Theta_{\text{CR}}(\xi^{\text{CR}}) \quad (\text{A9})$$

with

$$\xi^{\text{CR}} = F_{\theta}^{\text{GEA2+L}} - F_{\theta}^W - 1, \quad (\text{A10})$$

$$F_{\theta}^{\text{GEA2+L}} = 1 + b_1 s^2 + b_2 q \quad (\text{A11})$$

and the interpolation function

$$\Theta_{\text{CR}}(\xi) = \{1 - \exp[-1/|\xi|^a] [1 - H(\xi)]\}^{1/a}. \quad (\text{A12})$$

Here $H(\xi)$ is the Heaviside unit step function.

The original parameter values were $a = 4$ and (from the gradient expansion) $b_1 = \frac{5}{27}$, $b_2 = \frac{20}{9}$. The CR_{opt} values are $a = 4$, $b_1 = -0.295491$, $b_2 = 2.615740$ [9].

TFL_{opt}

The regularized Thomas-Fermi-plus-Laplacian enhancement function [44] is the combination of

$$F_t^{\text{TFL}} = 1 + \frac{20}{9}q \quad (\text{A13})$$

and the constraint to satisfy the von Weizsäcker lower bound

$$F_t^{\text{TFLreg}} = \max(F_t^{\text{TFL}}, F_t^{\text{vW}}). \quad (\text{A14})$$

For TFL_{opt} , the parameters to be optimized were the coefficients of the second-order gradient expansion, yielding

$$F_t^{\text{TFLopt}} = 1 + as^2 + bq, \quad (\text{A15})$$

with $a = -0.203519$ and $b = 2.513880$.

[1] “Reworking the Tao–Mo exchange-correlation functional: I. Reconsideration and Simplification”, H. Francisco, A.C. Cancio, and S.B. Trickey, preceding paper.

[2] M. Städele, J.A. Majewski, P. Vogl and A. Görling, Phys.

Rev. Lett. **79**, 2089 (1997)

[3] T. Grabo, T. Kreibich and E.K.U. Gross, Molec. Eng. **7**, 27 (1997).

[4] T. Grabo, T. Kreibach, S. Kurth, and E.K.U. Gross, in *Strong Coulomb Correlations in Electronic Structure: Beyond the Local Density Approximation*, V.I. Anisimov ed. (Gordon and Breach, Tokyo, 2000) 203.

[5] A. Heßelmann and A. Görling, Chem. Phys. Lett. **455**, 110 (2008) and refs. therein.

[6] Daniel Mejía Rodríguez and S.B. Trickey, Phys. Rev. B **102**, 121109(R) [4 pp] (2020).

[7] C. Lee, W. Yang, and R.G. Parr, Phys. Rev. B **37**, 785 (1988).

[8] J.P. Perdew, and L. Constantin, Phys. Rev. B **75**, 155109 (2007).

[9] D. Mejía-Rodríguez and S.B. Trickey, Phys. Rev. A **96**, 052512 (2017).

[10] D. Mejía-Rodríguez and S.B. Trickey, Phys. Rev. B **98**, 115161 (2018).

[11] J. Tao, J.P. Perdew, V.N. Staroverov, and G.E. Scuseria, Phys. Rev. Lett. **91**, 146401 [4 pp] (2003).

[12] J.P. Perdew, J. Tao, V.N. Staroverov, and G.E. Scuseria, J. Chem. Phys. **120**, 6898-6911 (2004).

[13] J. Tao and Yuxiang Mo, Phys. Rev. Letter. **117**, 073001 (2016).

[14] Subrata Jana, Kedar Sharma, and Prasanjit Samal J. Phys. Chem. A **123**, 6356 (2019).

[15] A. Patra, S. Jana and P. Samal, J. Chem. Phys. **153**, 184112 (2020).

[16] S. Jana, S.K. Behera, S. Śmiga, L. Constantin, and P. Samal, *v2-sregTM*, and *v2-sregTM-L* J. Chem. Phys. **155**, 024103 (2021).

[17] “Orbital-Free Density Functional Theory: An attractive electronic structure method for large-scale first-principles simulations”, Wenhui Mi, Kai Luo, S.B. Trickey, and Michele Pavanello, Chemical Reviews, provisionally accepted.

[18] T. Koga, K. Kanayama, S. Watanabe and A.J. Thakkar, Int. J. Quantum Chem. **71**, 491 (1999).

[19] A.J. Thakkar and T. Koga, in *Fundamental World of Quantum Chemistry: A Tribute to the Memory of Per-Olov Löwdin*, E.J. Brändas and E.S. Kryachko eds. (Kluwer Academic, Dordrecht, 2003) 587.

[20] J.A. Nelder and R. Mead, Comput. J. **7**, 308 (1965).

[21] E. Aprà, E.J. Bylaska, W.A. de Jong, N. Govind, K. Kowalski, T.P. Straatsma, M. Valiev, H.J.J. van Dam, Y. Alexeev, J. Anchell, V. Anisimov, F.W. Aquino, R. Atta-Fynn, J. Autschbach, N.P. Bauman, J.C. Becca, D.E. Bernholdt, K. Bhaskaran-Nair, S. Bogatko, P. Borowski, J. Boschen, J. Brabec, A. Bruner, E. Cauët, Y. Chen, G.N. Chuev, C.J. Cramer, J. Daily, M.J.O. Deegan, T.H. Dunning Jr., M. Dupuis, K. G. Dyall, G.I. Fann, S.A. Fischer, A. Fonari, H. Frücht, L. Gagliardi, J. Garza, N. Gawande, S. Ghosh, K. Glaesemann, A. W. Götz, J. Hammond, V. Helms, E.D. Hermes, K. Hirao, S. Hirata, M. Jacqueline, L. Jensen, B.G. Johnson, H. Jónsson, R.A. Kendall, M. Klemm, R. Kobayashi, V. Konkov, S. Krishnamoorthy, M. Krishnan, Z. Lin, R.D. Lins, R.J. Littlefield, A.J. Logsdail, K. Lopata, W. Ma, A.V. Marenich, J. Martín del Campo, D. Mejía Rodríguez, J.E. Moore, J.M. Mullin, T. Nakajima, D.R. Nascimento, J.A. Nichols, P.J. Nichols, J. Nieplocha, A. Otero-de-la-Roza, B. Palmer, A. Panyala, T. Pirojsirikul, B. Peng, R. Peverati, J. Pittner, L. Pollack, R.M. Richard, P. Sadayappan, G.C. Schatz, W.A. Shelton, D.W. Silverstein, D.M.A. Smith, T.A. Soares, D. Song, M. Swart, H.L. Taylor, G. S. Thomas, V. Tipparaju, D.G. Truhlar, K. Tsemekhman, T. Van Voorhis, Á. Vázquez-Mayagoitia, P. Verma, O. Villa, A. Vishnu, K.D. Vogiatzis, D. Wang, J.H. Weare, M.J. Williamson, T.L. Windus, K. Wolinski, A.T. Wong, Q. Wu, C. Yang, Q. Yu, M. Zacharias, Z. Zhang, Y. Zhao, and R.J. Harrison, J. Chem. Phys. **152**, 184102 (2020).

[22] E. V. R. de Castro and F.E. Jorge, J. Chem. Phys. **108**, 5225 (1998).

[23] L.A. Curtiss, K. Raghavachari, P.C. Redfern, and J.A. Pople, J. Chem. Phys. **106**, 1063 (1997).

[24] L.A. Curtiss, P.C. Redfern, K. Raghavachari, and J.A. Pople, J. Chem. Phys. **114**, 108 (2001).

[25] V.N. Staroverov, G.E. Scuseria, J. Tao, and J.P. Perdew, J. Chem. Phys. **119** 12129 (2003).

[26] V.N. Staroverov, G.E. Scuseria, J. Tao, and J.P. Perdew, J. Chem. Phys. **121** 11507 (2004).

[27] H. Peng, Z.-H. Yang, J.P. Perdew, and J. Sun, Phys. Rev. X **6**, 041005 (2016).

[28] F. Tran, J. Stelzl, and P. Blaha, J. Chem. Phys. **144**, 204120 (2016).

[29] F. Tran and P. Blaha, J. Phys. Chem. A **121**, 3318 (2017).

[30] M. A. L. Marques, M. J. T. Oliveira, and T. Burnus, Comput. Phys. Commun. **183**, 2272 (2012).

[31] G. Kresse and D. Joubert, Phys. Rev. **59**, 1758 (1999).

[32] Supplemental Information is provided at XXX.

[33] A.C. Cancio, D. Stewart and A. Kuna, J. Chem. Phys. **144**, 084107 (2016).

[34] J. Sun, A. Ruzsinszky, and J.P. Perdew, Phys. Rev. Lett. **115**, 036402 (2015).

[35] J. Sun, R.C. Remsing, Y. Zhang, Z. Sun, A. Ruzsinszky, H. Peng, Z. Yang, A. Paul, U. Waghmare, X. Wu, M.L. Klein, and J.P. Perdew, Nature Chemistry **8**, 831 (2016).

[36] J. P. Perdew, K. Burke, and M. Ernzerhof Phys. Rev. Lett **77**, 3865 (1996); erratum *ibid.* **78**, 1396 (1997).

[37] F. Weigend and R. Ahlrichs, Phys. Chem. Chem. Phys. **7**, 3297 (2005).

[38] H. Dana, A. Herr, and A.J.P. Meyer, J. Appl. Phys. **39**, 669 (1968).

- [39] H.P. Meyers and W. Sucksmith, Proc. R. Soc. A **207**, 427 (1951).
- [40] Kaplan, Aaron D. and Perdew, John P., Phys. Rev. Mater., **6**, 083803 (2022).
- [41] J. Sun, J.P. Perdew, and A. Ruzsinszky, Proc. Nat. Acad. Sci. (USA) **112**, 685 (2015).
- [42] D. Mejía-Rodríguez and S.B. Trickey, Phys. Rev. B **100**, 041113(R) (2019).
- [43] A.C. Cancio and J.J. Redd, Mol. Phys. **115**, 618 (2017).
- [44] S. Śmiga, E. Fabiano, L.A. Constantin and F. Della Sala, J. Chem. Phys. **146**, 064105 (2017).